Letters in Applied NanoBioScience
Open-Access Journal (ISSN: 2284-6808)

Article
Volume 15, Issue 1, 2026, 17
https://doi.org/10.33263/LIANBS151.017

Oligosaccharides as an Alternative Drug for COVID-19 – An In Silico Analysis

Aanandhalakshmi Raghuraman [1], Gowtham Palani Shanthi [1], Bazeera Ferdhous Proskhan [1], Vanavil Balakrishnan [1,*]

[1] Department of Biotechnology, Kalasalingam Academy of Research and Education, Krishnankoil-626126, Tamil Nadu, India
* Correspondence: b.vanavil@klu.ac.in;

Received: 30.10.2024; Accepted: 24.02.2026; Published: 30.03.2026

Abstract: COVID-19 is an infectious disease caused by Severe Acute Respiratory Syndrome Coronavirus 2 that keeps affecting the lives of several million people. It is the need of the hour to find a potential drug that prevents this viral infection, saving millions of lives worldwide. Studies have shown that sulphated polysaccharides possess anti-viral activities against dengue, malaria, HIV, and hepatitis B virus. Oligosaccharides have remarkable biological properties for maintaining human health and are being explored for their potential to treat diseases such as Parkinson's and Crohn's. In this perspective, the present study has focused on exploring the anti-viral nature of oligosaccharides against SARS-CoV-2 by molecular docking against the receptor-binding domains of COVID-19 target structural proteins using AUTODOCK, and the analysis was performed using ADMET and pkCSM tools to predict the toxicity properties of oligosaccharides. Docking results showed that oligomers derived from exopolysaccharides, such as Curdlan and dextran, and their sulphated derivatives, as well as sulphated polysaccharides of seaweed origin, such as fucoidan, carrageenan, and ulvan, had better binding affinity with the target proteins. The binding affinity for 10 units of oligomers of fucoidan with nucleocapsid receptor - binding domain was -11.5 (kcal/mol), followed by ulvan oligomers with -11.2 (kcal/mol). The 10 units of oligomers of fucoidan had a higher binding score with nucleocapsid receptor binding domains of COVID -19, followed by ulvan oligomers when compared to other sulphated oligosaccharides and control ligand. Further, the toxicity profiles of these oligomers, evaluated computationally, were found to be encouraging and safe with respect to toxicological aspects. Therefore, these bioactive oligosaccharides can be exploited as an effective anti-viral therapeutic mediator for SARS-CoV-2. This study will, to our knowledge, shed light on the application of oligosaccharides in developing a possible therapeutic intervention against COVID-19. This study is the first report to assess the potential of sulphated oligosaccharides for the development of anti-viral agents for COVID-19.

Keywords: COVID-19; carbohydrate drugs; oligosaccharides; toxicity analysis; drug design.

1. Introduction

COVID-19 is the recent pandemic caused by Severe Acute Respiratory Syndrome Coronavirus 2 (SARS-CoV-2) that threatens the whole world. The scientific community is researching worldwide to develop a potential strategy to combat this deadly disease and to present an effective cure for COVID-19. It is necessary in the current time to identify a potential

inhibitor that prevents this viral infection, saving millions of lives worldwide. Due to their advantages, including lower cost, abundance, diverse functional groups, and molecular structures, several bioactive carbohydrates have been explored as drugs, conjugates, scaffolds, vaccines, and glyconanomaterials [1]. Carbohydrate-based therapeutic interventions are used widely in cardiovascular and hematological treatments. Polysaccharides and oligosaccharides are employed as anti-inflammatory, anticoagulant, and antithrombotic agents [2] and as antimicrobial agents [3]. In addition, these molecules are being used as prebiotics [4]. In particular, Several bioactive compounds of different structural types have been identified from marine micro- and macro-organisms that inhibit both RNA and DNA viruses. These include polysaccharides, terpenes, steroids, alkaloids, and peptides [5]. Fucoidan, derived from brown macroalgae, could serve as a potential inhibitor by controlling the 3-chymotrypsin-like protease activity, hence preventing viral replication and effectively combating COVID-19 [6]. These functional molecules originate from different sources. Seaweeds and plants are a rich reservoir of diverse oligosaccharides. Some of the well-known bioactive oligosaccharides include isomaltooligosaccharides, glucooligosaccharides, fructooligosaccharides, galactooligosaccharides, and xylo-oligosaccharides [7]. Currently, carbohydrate-based drugs approved for the treatment of several diseases constitute only a minor share of the drugs available on the market [8]. To prevent the spread of influenza A and B, sialic acid analogs such as peramivir and laninamivir octanoate have been developed as neuraminidase inhibitors.

Additionally, since the natural carrageenans prevent viruses from attaching to and infecting host cells, the Iota-carrageenan carragelose was recently licensed as an over-the-counter medication [9]. Peptidomimetic oligomers can disrupt the lipid envelopes of viruses by interacting with the membrane, increasing permeability, or inducing lysis, thereby releasing vital viral components [10]. Microvirin monomers and oligomers have demonstrated significant antiviral activity against HCV, with oligomers, notably dimers and trimers, exhibiting superior neutralizing activity compared to monomers [11]. The ACE2 receptors and the gut microbiota play important roles in the pathogenesis of COVID-19 [12]. Oligosaccharides can alter gut flora and ACE2 expression, suggesting the potential significance of improving gut microbiota for post-COVID-19 management [11]. Molecular docking was used to calculate the binding affinities of human milk oligosaccharides with viral proteins [13]. Cyclodextrins, cyclic oligosaccharides, can enhance the solubility, stability, and absorption of antiviral drugs, while boosting their bioactivity and lowering their toxicity [14]. Molecular docking of drug targets with ligands facilitates the identification of specific binding sites and key interactions [15] and is also significant for determining the interaction mode of small compounds at the active site of the targeted receptor protein [16]. Screening drugs or inhibitors using molecular docking studies not only reduces the need for extensive clinical trials but also lowers drug discovery and development expenses. Heparin sulfate was found to display binding affinity to the spike protein of SARS CoV-2 [8]. 2-deoxy-D- glucose was employed in adjunctive therapy for COVID -19 [15]. Sulphated polysaccharides extracted from seaweeds have been testified to possess anti-viral properties [17]. Sulfated disaccharide lactulose octasulfate (LOS) exhibits strong anti-viral properties against coronaviruses [18]. The interaction between OP145, oligo-porphyran from *Pyropia yezoensis* (red seaweed), and the S-protein was simulated using molecular docking, and OP145 was effective in treating and preventing COVID-19 [19]. The use of oligosaccharides as a therapeutic agent for COVID-19 has not been explored well. This analysis can fuel the development of novel oligosaccharide-based therapeutic molecules to deal with SARS-CoV-2.

In this study, the focus was on the docking of the receptor-binding domains of SARS-CoV-2 target proteins with different oligosaccharides as ligands using a computational method. Further, the interacting amino acid**s in the receptor-binding domain of SARS-CoV-2 with** oligosaccharides and the toxicity of oligosaccharides were analyzed using an in silico approach.

2. Materials and Methods

2.1. Retrieval of target proteins and ligands.

Protein Data Bank was employed to retrieve the 3D structures of four receptor binding domains of SARS-CoV-2 target proteins, such as spike receptor binding domain (PDB: 7JVB), nucleocapsid protein N-terminal RNA binding domain (PDB: 6M3M), non-structural protein -1 (PDB: 6ZLW), and non-structural protein 5 (PDB: 7JP1), and are depicted in Figures 1a-1d. Chemsketch is used to draw the chemical structures of oligosaccharides of different chain lengths. All the oligosaccharides' three-dimensional structures were designed by sketching repeating units of monomers of respective polysaccharides. 3, 4, 5, and 10 units of oligomers were sketched to perform the analysis. Nirmatrelvir was taken as a control drug. The 3D structure of the control drug nirmatrelvir was retrieved from PubChem.

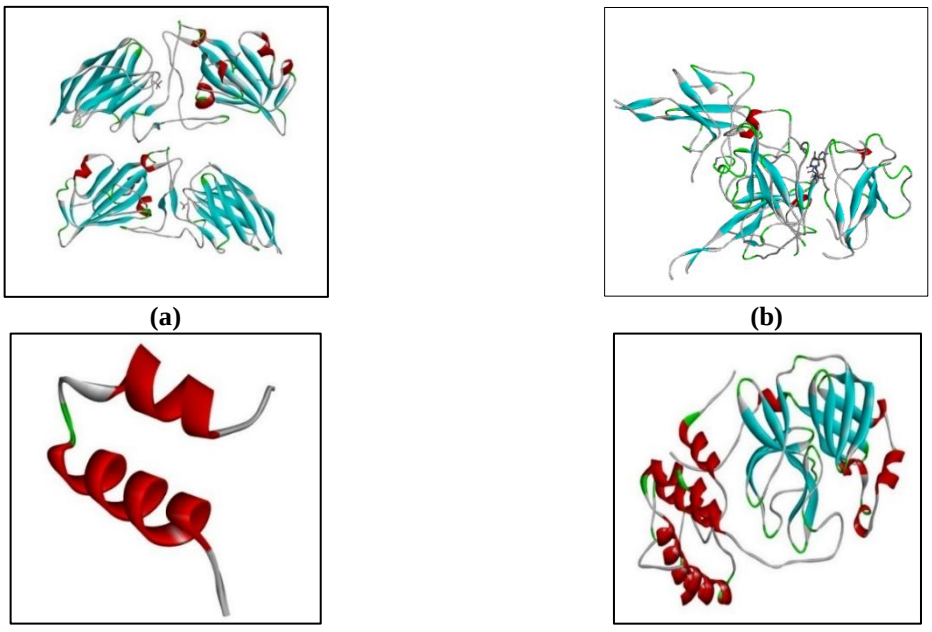

Figure 1. Structure of SARS-CoV-2 target proteins **(a)** Spike receptor-binding domain; **(b)** Nucleocapsid protein N-terminal RNA binding domain; **(c)** Non-structural protein – 1; **(d)** Non-structural protein – 5.

2.2. Docking of receptor-binding domain with oligosaccharides.

Docking of molecules was performed using AutoDock Vina (v1.5.6) [20,21]. Docking or binding scores were estimated in kcal/mol, and the more negative the score, the better the binding of ligands with the proteins. Before docking, polar-H atoms and Kollman charges were added to the receptor. The processed ligands were exported as PDB format, and Gasteiger charges were added to the ligands. Both the ligand and receptor files were then saved in pdbqt format. The grid box center for interaction between the control drug and targets was found to be 13.468, 1.58, 5.562; 14.482, -10.473, -23.232; 239.11, 215.479, 197.672; 12.641, 0.466, 4.919, respectively [22].

2.3. Amino acid interaction of receptor-binding domain with oligosaccharides.

After receiving the AutoDock results, the output was displayed in Discovery Studio to visualize the amino acid interactions between the receptor-binding domains of COVID-19 and the oligosaccharides [21]. The interacting amino acids were noted.

2.4. Toxicity analysis.

Toxicity and clinical safety are the foremost concerns in drug development. Toxicity is a substantial cause for failure in drug development [23]. Toxicity analysis was carried out using the ADMET tool [24, 25]. Initially, the oligosaccharide structures were converted into SMILES text format using SwissADME. Toxicological profiles of Curdlan, Dextran, Curdlan sulfate, Dextran sulfate, Fucoidan, Lambda Carrageenan, Kappa Carrageenan, and Ulvan were predicted using the pkCSM tool [26]. The toxicity of drugs was predicted based on AMES toxicity, hERG inhibition, acute toxicity, chronic toxicity, *T. pyriformis* toxicity, minnow toxicity, hepatotoxicity, and skin sensitization. The maximum recommended tolerated dose (MRTD) for each oligosaccharide was also predicted.

3. Results and Discussion

3.1. Docking of receptor-binding domain with oligosaccharides.

To analyse the interaction between oligosaccharides and target proteins of COVID-19, molecular docking was performed, and the 3D interaction visualization between oligosaccharides and target proteins of COVID-19 is represented from Figures 2 to 10, and the respective binding affinities were compared and are represented in Figure 12.

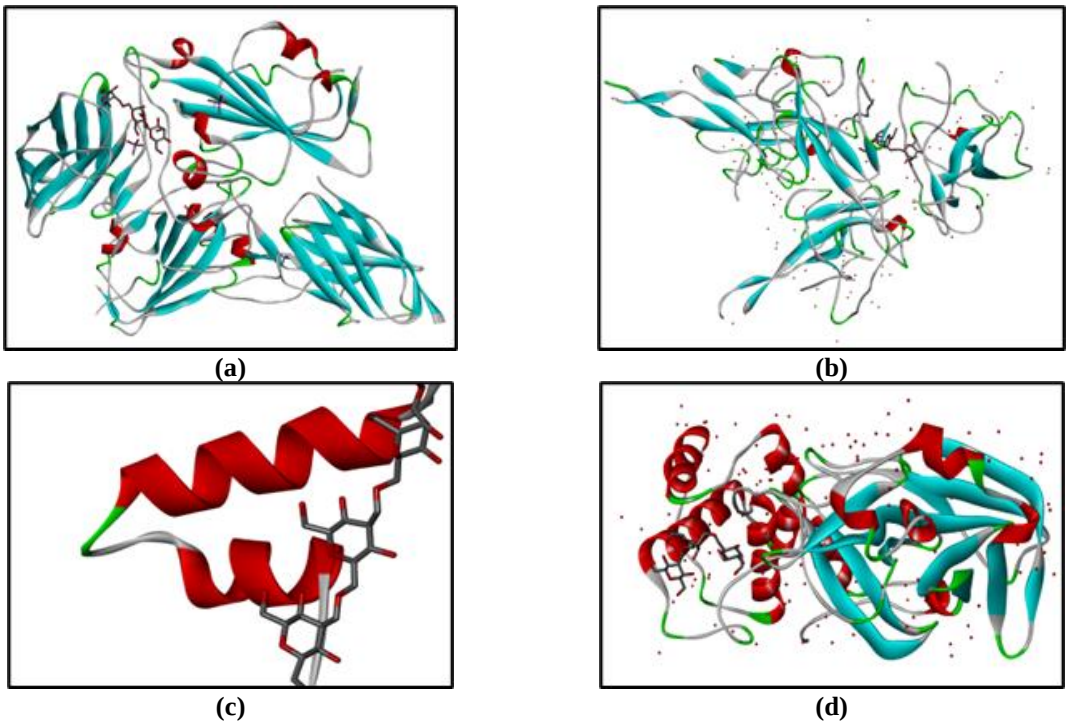

Figure 2. Docking of sulphated oligosaccharides (3 units) with COVID-19 receptor binding domain **(a)** Spike receptor binding domain vs Curdlan; **(b)** Nucleocapsid receptor binding domain vs Curdlan; **(c)** Non-structural protein - 1 vs Curdlan; **(d)** Non-structural protein - 5 vs Curdlan.

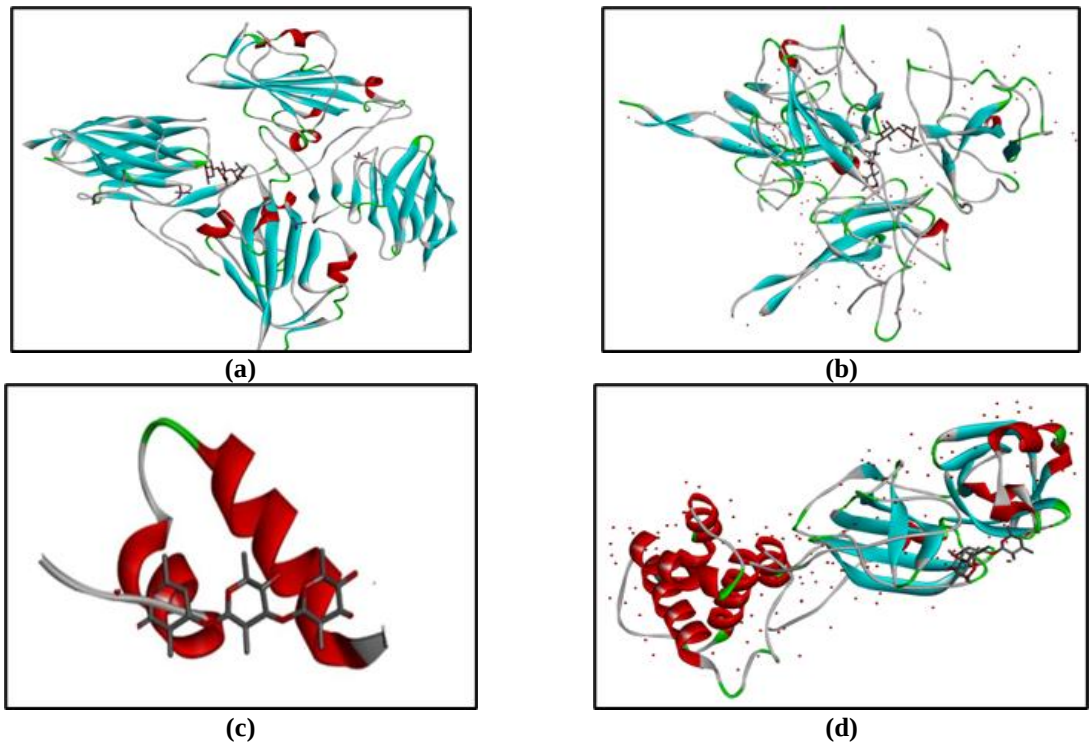

Figure 3. Spike receptor binding domain vs Fucoidan; **(a)** Nucleocapsid receptor binding domain vs Fucoidan; **(b)** Non Docking of sulphated oligosaccharides (5 units) with COVID-19 receptor binding domain **(c)** structural protein - 1 vs Fucoidan; **(d)** Non-structural protein - 5 vs Fucoidan.

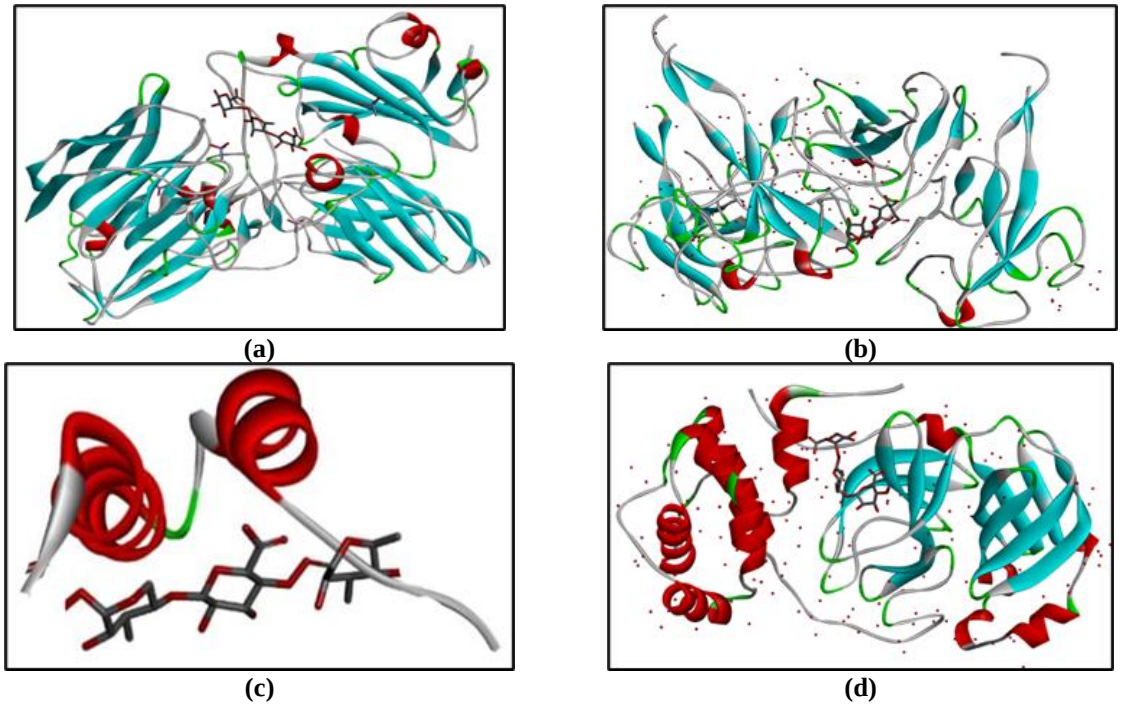

Figure 4. Docking of sulphated oligosaccharides (5 units) with the COVID-19 receptor binding domain **(a)** Spike receptor binding domain vs Ulvan; **(b)** Nucleocapsid receptor binding domain vs Ulvan; **(c)** Non-structural protein - 1 vs Ulvan; **(d)** Non-structural protein - 5 vs Ulvan.

After analyzing the binding affinity obtained by the different oligosaccharides with the four different receptor-binding domains of COVID-19, it was found that the binding affinity for fucoidan oligomers of 10 units and oligomers of ulvan with 10 units with the nucleocapsid receptor-binding domain were high (-11.5 and 11.2 kcal/mol). Concerning the binding of different oligosaccharides with the spike receptor binding domain, 10-unit

oligomers of fucoidan, followed by sulphated derivatives of Curdlan and dextran, were found to possess higher binding affinity.

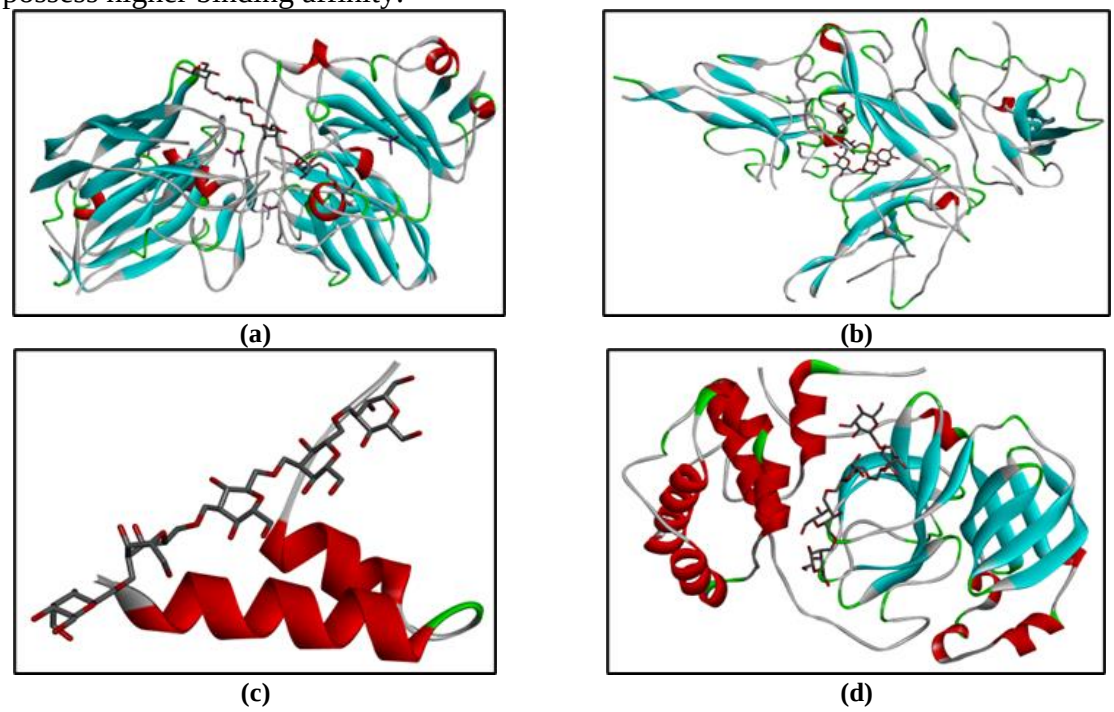

Figure 5. Docking of sulphated oligosaccharides (5 units) with the COVID-19 receptor binding domain **(a)** Spike receptor binding domain vs Curdlan; **(b)** Nucleocapsid receptor binding domain vs Curdlan; **(c)** Non-structural protein-1 vs Curdlan; **(d)** Non-structural protein-5 vs Curdlan.

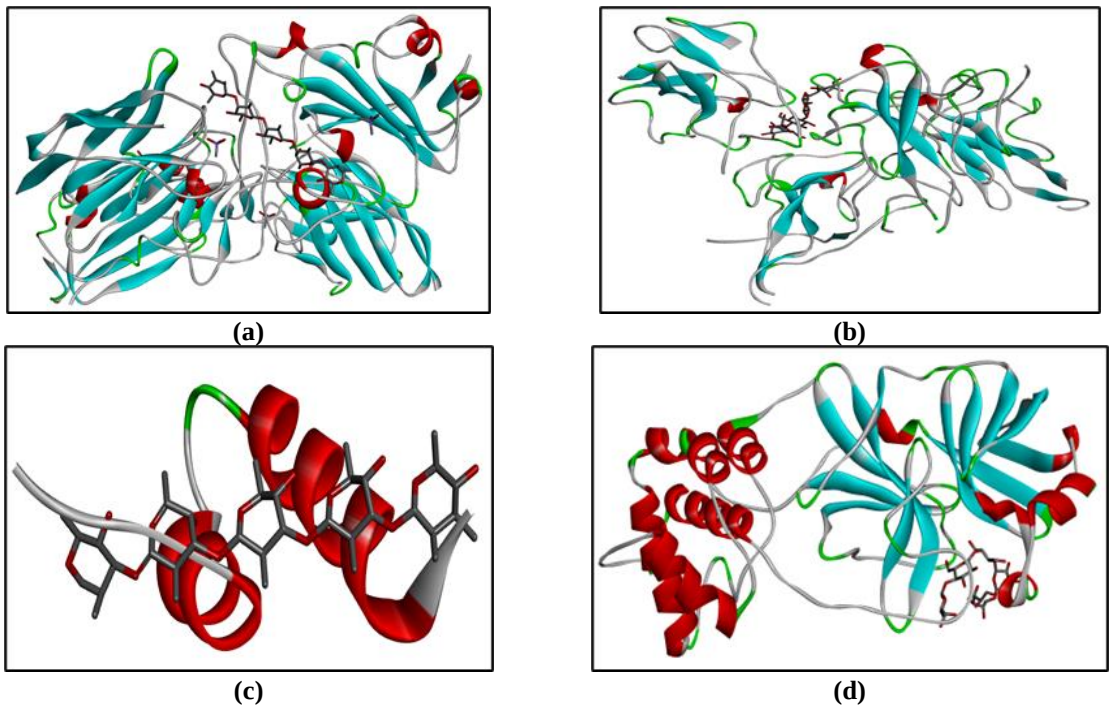

Figure 6. Docking of sulphated oligosaccharides (5 units) with the COVID-19 receptor binding domain **(a)** Spike receptor binding domain vs Fucoidan; **(b)** Nucleocapsid receptor binding domain vs Fucoidan; **(c)** Non-structural protein - 1 vs Fucoidan; **(d)** Non-structural protein - 5 vs Fucoidan.

Similar binding affinity was reflected in non- structural protein-1 of SARS-CoV-2 as well. It was observed that all units of ulvan have a high binding affinity with non- structural protein-1. The binding affinity showed that 10 units of fucoidan and ulvan with the nucleocapsid receptor-binding domain had higher affinity when compared to the control drug.

The 3D interaction visualization between the control drug and target proteins of COVID-19 is displayed in Figure 11.

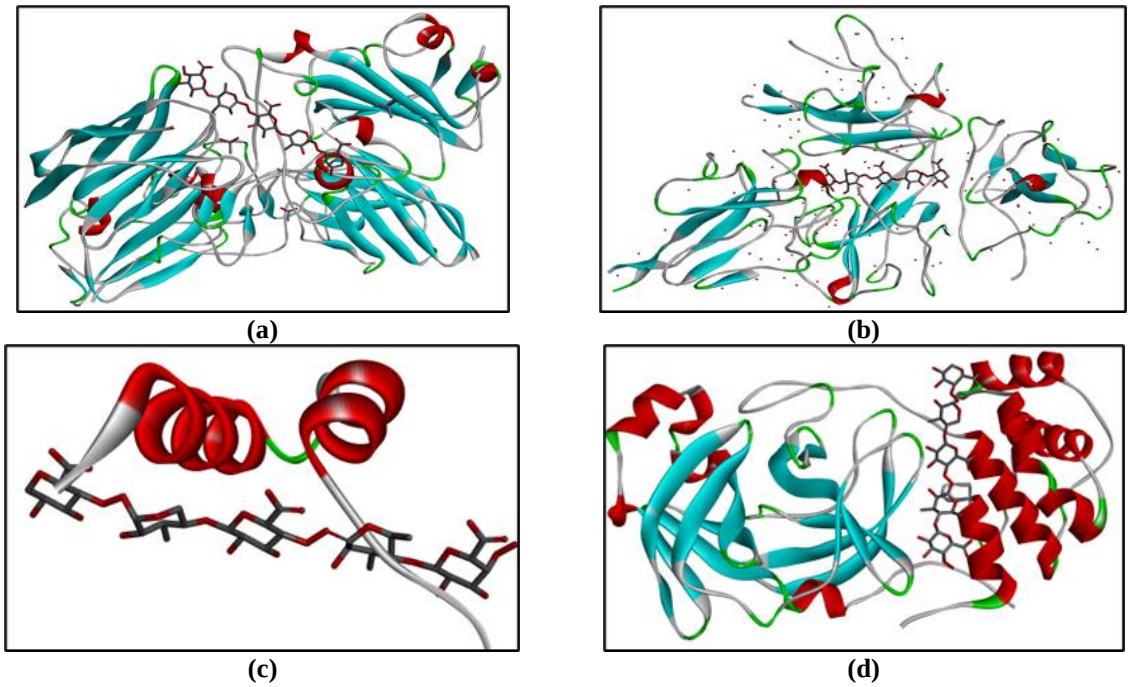

Figure 7. Docking of sulphated oligosaccharides (5 units) with the COVID-19 receptor binding domain **(a)** Spike receptor binding domain vs Ulvan; **(b)** Nucleocapsid receptor binding domain vs Ulvan; **(c)** Non-structural protein - 1 vs Ulvan; **(d)** Non-structural protein - 5 vs Ulvan.

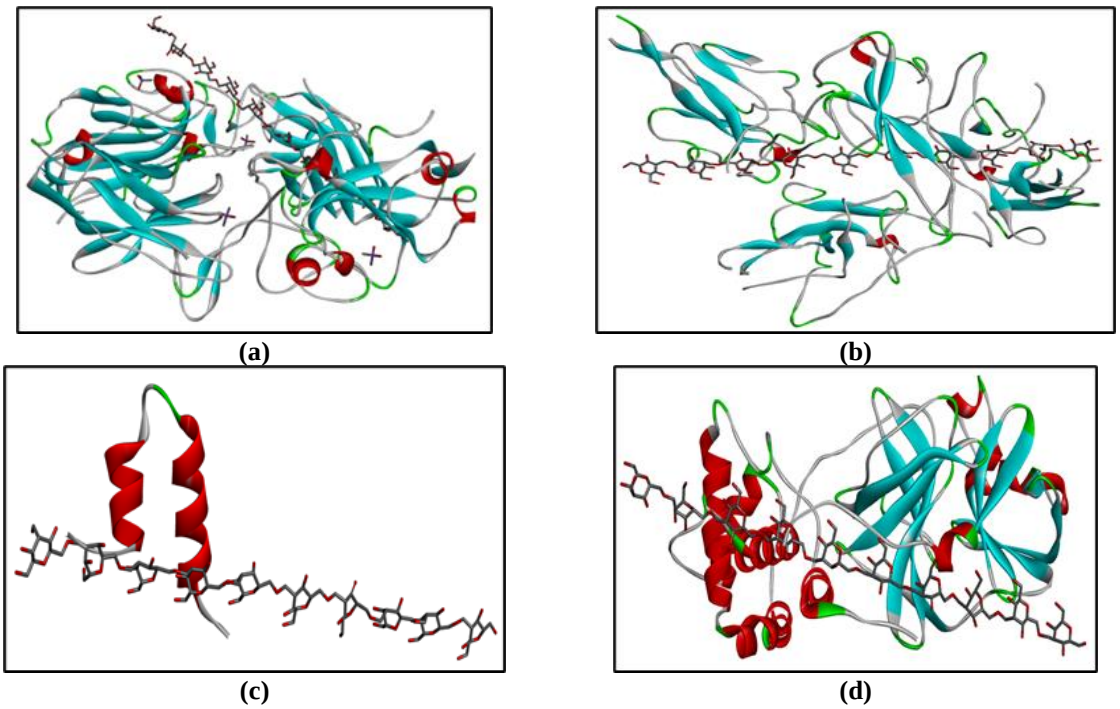

Figure 8. Docking of sulphated oligosaccharides (10 units) with COVID-19 receptor binding domain **(a)** Spike receptor binding domain vs Curdlan; **(b)** Nucleocapsid receptor binding domain vs Curdlan; **(c)** Non-structural protein - 1 vs Curdlan; **(d)** Non-structural protein - 5 vs Curdlan.

The control drug showed binding affinity with the spike receptor binding domain, nucleocapsid protein N-terminal RNA binding domain, non-structural protein - 1, non-structural protein – 5 as -4.77 kcal/mol, -2.59 kcal/mol, -3.46 kcal/mol, and -3.61 kcal/mol, respectively. Table 1 shows the binding energy of SARS-CoV-2 targets with the different ligand molecules.

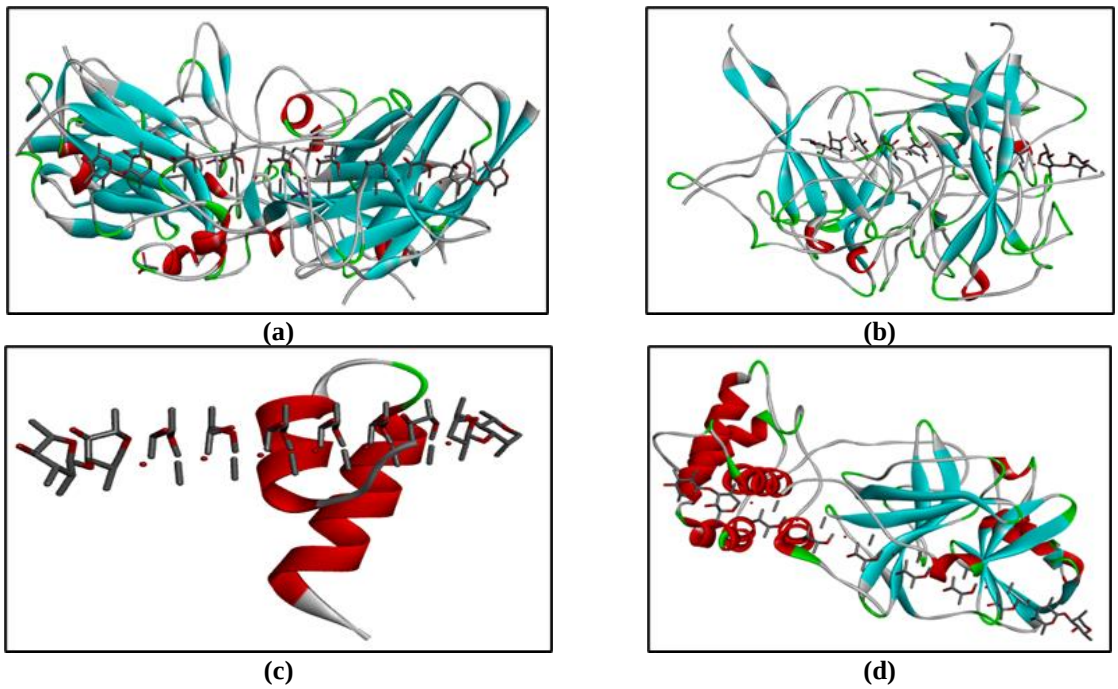

(a) **(b)** **(c)** **(d)**

Figure 9. Docking of sulphated oligosaccharides (10 units) with COVID-19 receptor binding domain **(a)** Spike receptor binding domain vs Fucoidan; **(b)** Nucleocapsid receptor binding domain vs Fucoidan; **(c)** Non-structural protein-1 vs Fucoidan; **(d)** Non-structural protein-5 vs Fucoidan.

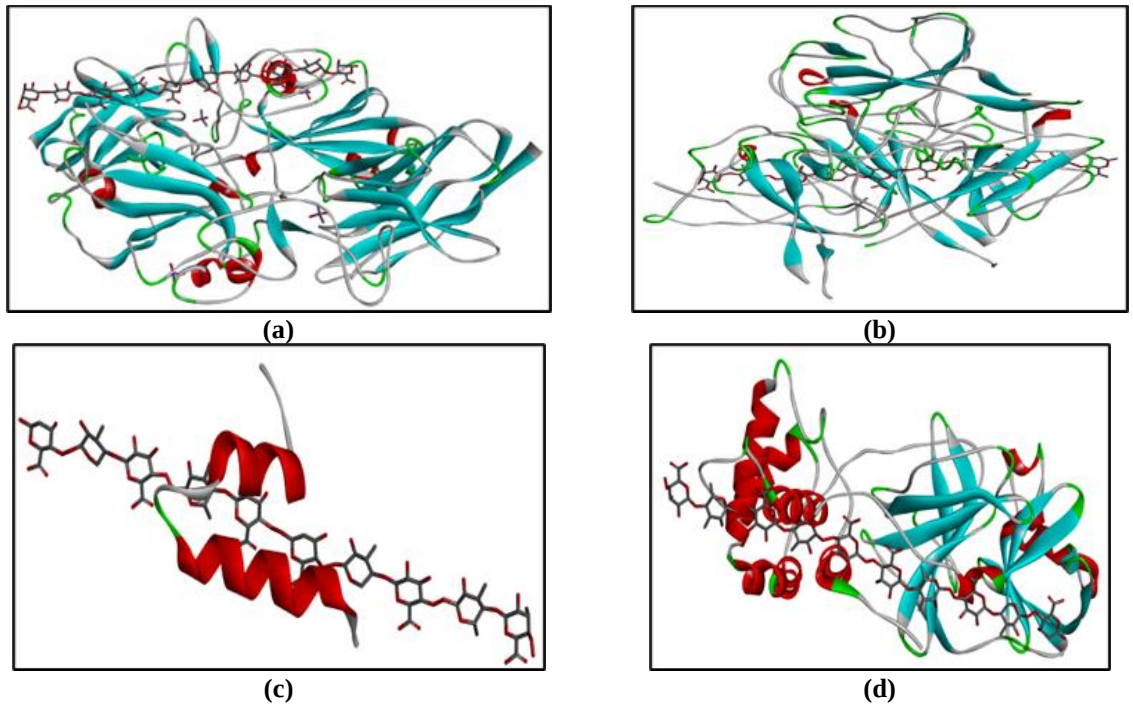

(a) **(b)** **(c)** **(d)**

Figure 10. Docking of sulphated oligosaccharides (10 units) with the COVID-19 receptor binding domain **(a)** Spike receptor binding domain vs Ulvan; **(b)** Nucleocapsid receptor binding domain vs Ulvan; **(c)** Non-structural protein - 1 vs Ulvan; **(d)** Non-structural protein - 5 vs Ulvan.

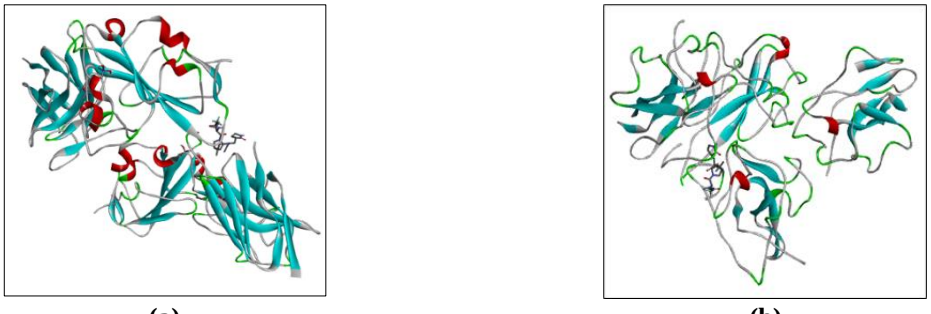

(a) **(b)**

(c) **(d)**

Figure 11. Docking of nirmatrelvir with COVID-19 receptor binding domain **(a)** Spike receptor binding domain; **(b)** Nucleocapsid receptor binding domain; **(c)** Non–structural protein–1; **(d)** Non–structural protein–5.

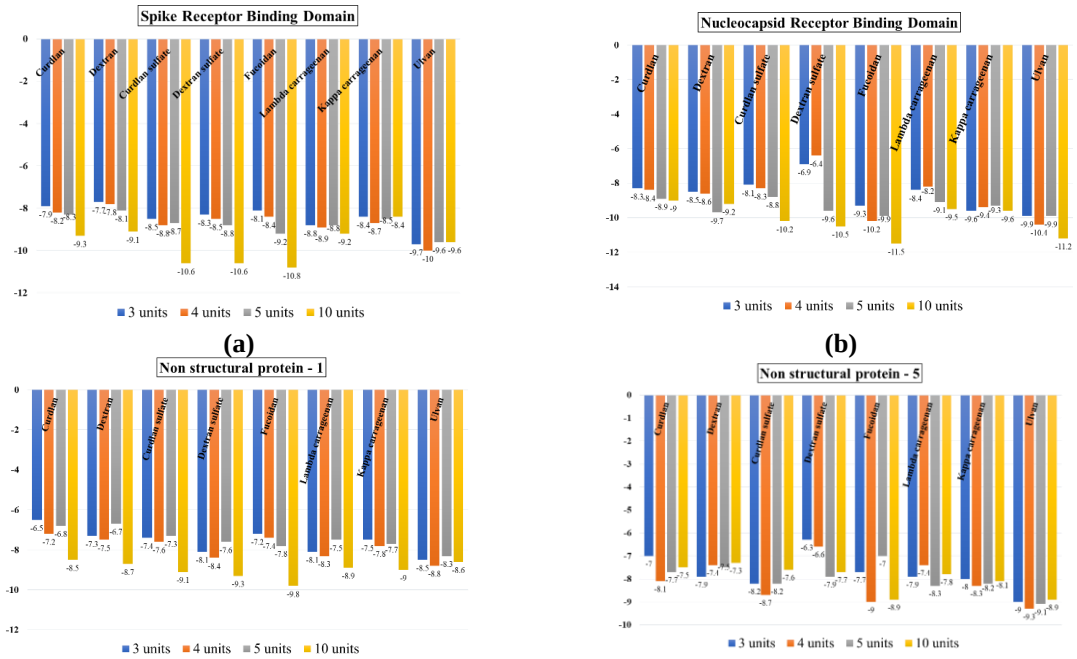

(a) **(b)**

(c) **(d)**

Figure 12. Binding energy (in kcal/mole) for all oligomeric ligand molecules against **(a)** Spike receptor-binding domain of SARS-CoV-2; **(b)** Nucleocapsid receptor- binding domain of SARS-CoV-2; **(c)** Non-structural protein-1 of SARS-CoV-2; **(d)** Non- structural protein-5 of SARS-CoV-2.

Table 1. Binding energy of SARS-CoV-2 targets with the ligand molecules.

S. no	Ligand	Docking affinity (– kcal/mole)															
		Spike receptor binding domain				Nucleocapsid receptor binding domain				Non-structural protein-1				Non-structural protein-5			
		(Number of units)															
		3	4	5	10	3	4	5	10	3	4	5	10	3	4	5	10
1	Curdlan	-7.9	-8.2	-8.3	-9.3	-8.3	-8.4	-8.9	-9.0	-6.5	-7.2	-6.8	-8.5	-7.0	-8.1	-7.7	-7.5
2	Dextran	-7.7	-7.8	-8.1	-9.1	-8.5	-8.6	-9.7	-9.2	-7.3	-7.5	-6.7	-8.7	-7.9	-7.4	-7.5	-7.3
3	Curdlan sulfate	-8.5	-8.8	-8.7	-10.6	-8.1	-8.3	-8.8	-10.2	-7.4	-7.6	-7.3	-9.1	-8.2	-8.7	-8.2	-7.6
4	Dextran sulfate	-8.3	-8.5	-8.8	-10.6	-6.9	-6.4	-9.6	-10.5	-8.1	-8.4	-7.6	-9.3	-6.3	-6.6	-7.9	-7.7
5	Fucoidan	-8.1	-8.4	-9.2	-10.8	-9.3	-10.2	-9.9	-11.5	-7.2	-7.4	-7.8	-9.8	-7.7	-9.0	-7.0	-8.9
6	Lambda Carrageenan	-8.8	-8.9	-8.8	-9.2	-8.4	-8.2	-9.1	-9.5	-8.1	-8.3	-7.5	-8.9	-7.9	-7.4	-8.3	-7.8
7	Kappa Carrageenan	-8.4	-8.7	-8.5	-8.4	-9.6	-9.4	-9.3	-9.6	-7.5	-7.8	-7.7	-9.0	-8.0	-8.3	-8.2	-8.1
8	Ulvan	-9.7	-10.0	-9.6	-9.6	-9.9	-10.4	-9.9	-11.2	-8.5	-8.8	-8.3	-8.6	-9.0	-9.3	-9.1	-8.9
9	Nirmatrelvir (Control drug)	-4.77				-2.59				-3.46				-3.61			

3.2. Amino acid interaction of receptor-binding domain with oligosaccharides.

Amino acid interaction of four receptor binding domains of SARS-CoV-2 with each oligomeric ligand is tabulated in Tables 2 to 9. By analyzing the amino acid interactions of receptor-binding domains with oligosaccharides of different units, some of the amino acids present in the receptor-binding domains were found to be common. In the case of the spike receptor-binding domain, amino acids such as ARG403, GLY496, LYS417, GLN498, ASN501, and TYR505 are commonly found interacting with some oligomers. Moreover, ARG403 was reported as the primary component that interacts with the saccharide chain's sulfate/carboxyl groups [27]. In the N-terminal RNA-binding domain, the HIS146, ASN76, ASN151, and THR149 residues are involved in some of the oligosaccharide interactions. In the case of Nsp-5, residues such as GLN110, PHE294, SER158, CYS145, and PRO9 are commonly observed to interact with different oligosaccharides. In the case of Nsp-1, residues such as HIS165 and ASP156 are typically found interacting with different oligosaccharides.

Table 2. Amino acids of the receptor-binding domain of SARS-CoV-2 interacting with curdlan oligomers.

S. no	Ligand	Receptor	Units	Interacting amino acids
1.	Curdlan	Spike receptor-binding domain	3	ASN501, GLY496, ARG403, LYS417, GLN409
			4	LYS417, ASP405, ARG403, TYR505, TYR453, ILE99, ASN501, GLN498, GLY496, GLY446, GLY26, TYR449, GLY28, ALA27
			5	GLY446, TYR449, GLY28, GLY26, GLN498, GLY496, TYR505, ARG403, ASP405, GLN409, ARG408
			10	ALA27, GLU28, HIS30, ASN75, ALA73, TRY449, ARG403, GLN409, THR416, GLU516, LEU517
2.		Nucleocapsid receptor-binding domain	3	ASP145, THR149, THR77, ILE158, ASN76, ASN78, ASN155, ASN151, ASN127
			4	ASN155, THR149, THR77, ASN49, ASN127, HIS146, GLY125
			5	GLY125, THR149, ASN76, ASN155, ASN78, ASN49, TYR124, TRP133, LYS128
			10	ASN78, ASN49, ASN151, THR149, ASN154, ASN155, ARG108, TYR110, TYR112, ARG108, ALA51, ARG150, THR50
3.		Nsp-5	3	GLU166, LEU141, SER46, ASN142, SER144, GLY143, CYS145, THR25, THR24
			4	GLU166, HIS163, GLN189, HIS41, SER144, CYS145, ASN142, HIS41, SER46, THR26, THR25
			5	TYR154, ILE152, THR25, SER158, THR111, PRO108, HIS246
			10	GLN306, PRO108, LYS97, PRO9, ALA7, GLN299, GLY215, ASN142
4.		Nsp-1	3	ASP156, ILE119
			4	ASP156, THR151, ILE119, ARG171, HIS165, LYS164, SER167
			5	GLU176, GLY150, ARG175, HIS165
			10	GLU176, GLY179, ASP156, THR151, ILE119

Table 3. Amino acids of the receptor-binding domain of SARS-CoV-2 interacting with dextran oligomers.

S. no	Ligand	Receptor	Units	Interacting amino acids
1	Dextran	Spike receptor-binding domain	3	ASN481, CYS335, LEU335, CYS361, ASP364
			4	GLN174, CYS361, ASN481, ILE472, THR56, LYS63, ASP60
			5	LYS417, GLN409, TYR453, ARG403, ILE99, TYR505, TYR449, GLY496, ALA29, HIS30, ASN501, GLN498, GLY28, ARG76, ASN481, ILE472, ASN75, GLY26
			10	PHE464, GLU465, LYS417, LYS458, SER469, GLU417, ILE472, GLN174, CYS361, ASN481, GLY482, ASP60, SER61, GLU44, GLN87
2		Nucleocapsid receptor-binding domain	3	LEU160, GLN161, LEU162, THR166, GLY165, TYR173, GLY125, GLN84, GLN164, SER79, ASN76
			4	TYR173, TYR112, ARG150, ASN76, SER79, ARG108, LYS66, ARG93, ALA157
			5	ASN127, HIS146, GLY125, ASP83, ASN49, SER80, ASN78, THR77, ASN76, THR166, VAL159, ASP145

S. no	Ligand	Receptor	Units	Interacting amino acids
			10	HIS146, ILE147, SER80, ASN76, ALA157, ARG150, TYR110, TYR112, ARG89, ARG69, LYS66, ASP64, LYS128, TYR124
3		Nsp-5	3	HIS163, GLU166, GLN189, CYS145, SER144, ASN142, HIS41, SER146, THR26, THR25
			4	PHE8, ARG298, THR292, GLN110, PHE294, ASN142, SER158
			5	THR25, THR24, THR26, HIS41, GLN189, GLY143, CYS145, ASN142, LEU141, MET165, HIS163, GLU166
			10	GLY11, ASN142, GLN306, PHE294, PRO9, VAL303, ALA7, MET165, CYS300, SER158, GLY2, ASN214, GLY215
4		Nsp-1	3	HIS165, ASP156, GLY168, ARG171
			4	ARG171, GLU172, HIS165, ASP156
			5	ARG171, SER167, HIS165, ASP156, THR151
			10	ARG171, ASP156, GLU155, HIS165, GLU176, GLY180

Table 4. Amino acids of the receptor-binding domain of SARS-CoV-2 interacting with curdlan sulfate oligomers.

S. no	Ligand	Receptor	Units	Interacting amino acids
1.	Curdlan sulfate	Spike receptor-binding domain	3	ARG403, GLU406, LYS417, GLU100, ILE99, TYR449, GLY496, GLN498, GLY26, GLN1, TYR106
			4	ARG408, GLN409, GLU406, ARG403, TYR505, GLU100, GLN498, TYR449, ASN501, GLY496, ILE99, HIS30, GLY446, GLU98, GLN1, SER52, GLY26
			5	SER52, GLY54, MET55, GLU406, THR170, ILE468, TYR505, SER349, TYR451, ASN450, LYS144, THR345, ARG346, ARG509
			10	GLU516, ASP428, PRO463, GLU406, LYS417, ARG466, ASP467, ARG457, LYS144, SER349, GLU471, ILE172, GLN1, PRO479, CYS480, ASN481, CYS488, GLY496, ASP60, SER52, GLU44, ARG346, GLY446, PRO86
2.		Nucleocapsid receptor-binding domain	3	LYS103, ARG93, LEU105, HIS60, SER10, TYR173, ARG93, SER10, ARG108, THR58, ALA174, ALA157
			4	TYR112, ARG150, THR58, SER52, ALA157, ALA56, TYR110, ARG89, PRO118, ARG108,LYS66, ARG93, ASP64
			5	ARG108, ASN482, ASP129, ARG90, ASN155, ARG89, LYS66, TYR112, THR50, ALA51, TYR110, TYR173, THR55, ALA157, ALA56, ARG150
			10	THR58, ARG90, ASP64, ASP129, LYS66, ALA56, TYR110, ALA157, ARG150, THR50, ALA56, TYR112,
3.		Nsp-5	3	ARG131, LYS137, ASP289, LYS5, THR199, LEU287, LEU286, TYR239, TYR237, LEU272
			4	HIS172, CYS128, THR199, ASP197, GLN126, ASP289, GLU288, LYS5, THR239, GLN117
			5	LYS137, GLU14, GLY11, SER10, PRO9, PHE305, GLY302, GLY2, SER1, ASP197, ILE213
			10	ASP92, THR199, ASN95, VAL73, GLN74, GLY11, GLY15, LYS137,GLU14, SER1, PRO9, THR304, ILE213, SER10
4.		Nsp-1	3	ASP152, GLU155, GLN158, GLU159, LEU149, GLY180
			4	ARG175, GLY180, GLY179, GLU176, GLU172, PRO153, ASP152, ASP156, GLU155, THR151
			5	ARG175, ARG171, GLY168, SER167, HIS165, ASP156
			10	GLU155, ASP156, ARG171, GLU176, THR151, LEU149, GLU172, GLY179

Table 5. Amino acids of the receptor-binding domain of SARS-CoV-2 interacting with dextran sulfate oligomers.

S. no	Ligand	Receptor	Units	Interacting amino acids
1.	Dextran sulfate	Spike receptor-binding domain	3	GLY446, GLN498, TYR449, GLY26, ALA27, VAL2, GLN1, HIS30, ASP98, ILE99, GLU100, LYS417, GLY496, ARG403
			4	TYR106, GLN1, GLY26, ASP98, GLU100, GLY496, ASN501, TYR449, PHE497, GLN498, ARG403, TYR453, LYS417
			5	GLN498, ASN501, TYR449, GLY26, GLY496, ARG403, VAL2, GLN1, ASP98, GLU100, GLU406, GLN409, LYS417, GLY446, THR415
			10	GLU465, LYS462, SER459, LYS458, ARG403, ASP467, SER469, GLU471, ILE472, ASN501, CYS480, PRO479, GLY496, ASP98, LEU59, SER61, GLY26, ARG36, PRO39, GLY40, LYS41
2.		Nucleocapsid receptor-	3	LEU162, GLY70, GLU137, THR136, GLN71
			4	ASN76, ASN78, ASN49, HIS146, THR136

S. no	Ligand	Receptor	Units	Interacting amino acids
		binding domain	5	TYR112, TYR110, ARG150, THR136, VAL159, ARG69, ILE132, ILE131, LYS66, ASP64, ARG89, ARG90, ASN76, GLY130, LYS128
			10	GLY130, ARG90, GLY125, ASN49, ALA153, ASP64, LYS66, ARG69, ARG150, ASN78, HIS146, ALA156, ALA157, TYR110, ARG89, LYS128, LYS62, THR136
3.		Nsp-5	3	THR292, GLN110, PHE294, ARG298, ASN151, SER158, PHE8
			4	THR292, GLN110, THR111, ARG298, PHE8, ASN151, SER158
			5	HIS162, SER158, GLY124, SER123, TYR126, LYS137, ASN133, ASN151, ASP197, LYS5, ARG298, TYR239, TYR237, GLU288, LEU287, SER284
			10	ALA70, GLY71, GLU14, GLY11, SER123, VAL125, PRO9, ALA7, ARG4, GLY124, PHE8, GLY124, ASN214, THR292, ASN151
4.		Nsp-1	3	HIS165, GLY168, ARG171, VAL169, ASP156, GLU155, GLU169, GLY150
			4	GLU148, GLY150, THR151, ASP156, ARG171, GLY168, HIS165, GLU155, GLU159
			5	LEU149, GLY150, ASP156, GLU155, PRO153, GLU172, ARG171, ARG175, GLU76, GLY168, GLY180
			10	GLU148, LEU149, ASP156, ASN160, HIS165, SER167, ARG171, GLU172

Table 6. Amino acids of the receptor-binding domain of SARS-CoV-2 interacting with fucoidan oligomers.

S. no	Ligand	Receptor	Units	Interacting amino acids
1.	Fucoidan	Spike receptor-binding domain	3	GLY496, TYR58, TYR495, ARG403, TYR453, LEU99, GLU100, LYS417
			4	PRO479, CYS480, ILE472, ASN481, GLY132, TYR58, LYS63, ASN57, THR56, ARG403
			5	LYS417, GLN409, ARG408, TYR453, ARG403, TYR505, LEU99, ALA29, ASN57, GLN498, GLU26
			10	PRO39, LYS417, ALA29, GLN87, PRO86, GLY482, ASN481, CYS480, GLU471, ILE472, LYS458, GLU465, LYS462
2.		Nucleocapsid receptor- binding domain	3	THR149, THR77, ASN127
			4	ASN127, THR149, TRP53, ALA156, ILE158, HIS146, ILE147
			5	ASN155, ASN151, THR77, ASN76, ASN78, ASN49, GLY125, HIS146, THR149, ASN155, ALA156, GLY148
			10	THR50, ASN151, PRO118, ARG89, LYS66, ALA91, ARG108, TYR110, ALA157, ALA156, ARG89
3.		Nsp-5	3	VAL202, GLN110, PRO293, PHE294
			4	VAL202, HIS246, ASP245, PRO299, GLN110, PHE294
			5	CYS44, CYS145, SER46, GLN110, ASP245, LEU41, GLN189
			10	ILE213, GLN299, MET6, VAL303, PRO299, SER46, GLY11, GLY15, LYS97, PRO96, VAL202
4.		Nsp-1	3	ASP156, HIS165, GLY168
			4	VAL169, HIS165, GLY168, ASP156
			5	ARG175, PRO153, LEU149, ASP156
			10	LYS164, HIS165, SER167, ASP156, GLY150, LEU149

Table 7. Amino acids of the receptor-binding domain of SARS-CoV-2 interacting with kappa carrageenan oligomers.

S. no	Ligand	Receptor	Units	Interacting amino acids
1.	Kappa carrageenan	Spike receptor-binding domain	3	PHE338, VAL367, TYR365, CYS336, ASP364, ALA363, LEU513
			4	PHE338, VAL367, TYR365, CYS336, ASP364, ALA363, LEU513
			5	ARG408, GLN409, THR415, ARG403, TYR505, ASN501, TYR365, CYS336, ILE99, GLY28, TYR449
			10	TYR351, ILE99, THR470, TYR451, PHE347, ARG346, THR345, ASP364, LEU44, ARG403, ASN501, LYS63
2.		Nucleocapsid receptor- binding domain	3	GLN84, VAL76, PRO74, GLN71, SER79, GLY165, GLU137, PRO81, PRO163, LEU162
			4	THR116, THR149, ILE158, GLY165
			5	GLY165, THR149, TRP53, ALA156, ASN155, ASN78, ALA126, GLY125, TRP133, ILE158, LYS128,
			10	PHE54, THR149, ALA156, ARG108, VAL159, LYS66, TYR110, THR116
3.		Nsp-5	3	GLU166, HIS163, CYS145, SER46, HIS41, THR25, THR26
			4	ASN151, ASP295, THR111, CYS145, GLN110, THR292
			5	GLU240, GLN110, PRO108, GLN107, ASP295, ARG298, ASP153, SER158, LYS102

S. no	Ligand	Receptor	Units	Interacting amino acids
			10	PRO241, HIS246, GLU240, GLY107, PRO108, PHE294, ASP153, THR25, TYR154, ILE152, PHE305
4.		Nsp-1	3	GLU172, ASP156, LEU149, GLY150
			4	VAL169, GLU172, THR151
			5	ARG175, GLY150, GLU172, THR151, LEU149
			10	GLY150, ARG175, GLU172, THR151, GLY180, GLU148

Table 8. Amino acids of the receptor-binding domain of SARS-CoV-2 interacting with lambda carrageenan oligomers.

S. no	Ligand	Receptor	Units	Interacting amino acids
1.	Lambda carrageenan	Spike receptor-binding domain	3	GLN409, ASP405, ARG403, TYR505, GLN498, TYR495, ALA29, ILE99, TYR453, LYS417
			4	GLN498, ASN501, TYR505, ARG403,ASP405, GLN409, LYS417, TYR453, ILE99, ALA29, GLY28, TYR449, GLY26, ASN75
			5	ASN75, ASN72, GLY28, GLN498, TYR449, ALA29, GLY496, TYR505, ARG403, TYR453, ILE99, LYS417, GLN409
			10	TRP107, GLY28, ARG403, PHE486, VAL483, GLY482, ASN72, ALA29, GLY339, TRP353, ASN354, ARG355
2.		Nucleocapsid receptor-binding domain	3	ALA156, ASN155, THR149, ASN78, ASN27, LYS128, ALA126, ILE131, ILE132
			4	TYR124, GLY125, ASN127, ASN155, THR149, VAL159, GLY148, HIS146
			5	ARG69, GLY125, ASN127, ASN155, ASN49, ASN151, ASN78, TRP53, ILE158, ASN76
			10	GLY125, SER79, ALA153, PRO152, ARG69, ALA126, ALA157, VAL159, ARG108, HIS60, ILE131, ARG96
3.		Nsp-5	3	GLU240, ASN203, GLN110, THR111, ASN151, VAL104
			4	HIS246, VAL202, ILE249, PRO293, ASP295, GLN110, THR111, ASN151, ILE152
			5	PRO108, GLN107, ARG105, SER158, ILE152, THR111, GLN110, PHE294, ASP295, ARG298
			10	TYR154, THR304, VAL202, ASN151, ARG298, PHE294, PRO132, ASN203, GLU240, MET235, PRO108
4.		Nsp-1	3	ARG175, VAL169, GLY168, HIS165, LEU149
			4	ARG175, PRO153, LEU149
			5	GLU148, LEU149, ASP152, PRO153, GLU176, GLY179
			10	GLY179, GLU176, ARG175, GLU172, HIS165

Table 9. Amino acids of the receptor-binding domain of SARS-CoV-2 interacting with ulvan oligomers.

S. no	Ligand	Receptor	Units	Interacting amino acids
1.	Ulvan	Spike receptor-binding domain	3	ARG403, TYR505, ASN501, GLY496, TYR453, ILE99
			4	ARG403, TYR505, LYS117, ILE99, GLY496, GLN498, TYR449, GLY28, ALA2, GLY26
			5	ASN75, GLY26, ALA27, GLY28, HIS30, ALA2, TYR449, ASN501, GLN498, TYR505, ARG403, TYR453, LYS117, GLY416, THR415, GLN409, ARG408
			10	PRO86, GLN498, PRO39, ARG36, GLU44, SER61, ASP60, GLY496, ASN501, ILE472, CYS480, GLU471, ARG457, LYS458, SER459, PRO463, LYS117
2.		Nucleocapsid receptor- binding domain	3	HIS146, GLY148, GLN167, ASN76, THR77, TRP53, ASN49, ASN127
			4	GLY148, GLU107, LEU162, LEU160, LEU168, THR77, LEU57
			5	TYR110, ARG89, ARG90, ILE131, ASP129, LYS62, LYS66, GLN71, GLN167, THR77
			10	GLN167, LEU162, VAL159, ALA174, THR55, ALA157, ARG89, ARG90, TYR173, LEU160, GLN71, GLY148, THR166, PRO81, SER79, THR77
3.		Nsp-5	3	GLU166, MET165, HIS146, HIS163, CYS145, GLY145, ASN142
			4	VAL202, PRO293, HIS146
			5	ILE152, VAL303, ARG298, PHE294, THR292, GLN110, GLY109, PRO108, HIS146, GLU240
			10	PRO96, LYS97, GLY15, GLU14, PRO9, PHE294, THR304, VAL303,CYS145, SER1, ILE152
4.		Nsp-1	3	HIS165, ASP156, GLY150
			4	VAL169, ARG171, GLU155, ASP156, GLY150, LEU149
			5	GLU155, ASP152, ASP156, GLU176, GLU172, ARG171
			10	PRO153, GLU176, ARG171, GLU172, HIS165, LYS164

3.3. Toxicity analysis.

The toxicity analysis of oligosaccharides was performed, and the results are tabulated in Tables 10-13. The toxicity predicted from the AMES test implied that all molecules were non-mutagenic. Toxicity was witnessed for all oligosaccharides in *Tetrahymena pyriformis*. None of the units was found to be an hERG-I inhibitor; however, Curdlan, dextran, lambda, and kappa carrageenan were predicted to inhibit hERG II. None of the units has been predicted to induce hepatotoxicity. Further, all tested oligosaccharides of different units were categorised as 'low probability for acute toxicity' as the LD50 values were above 50 mg/kg [28]. Further, none of the oligomers were predicted to be connected with skin sensitization. The predicted MRTD values for different oligosaccharide units were low (<0.477 log (mg/kg/day)) and indicated low toxicity, and high (>0.477 log (mg/kg/day)) indicated high toxicity. Oral rat chronic studies help to identify the lowest dose of a metabolite that results in an observed adverse effect. For tested oligomers, the predicted log Lowest Observed Adverse Effect (LOAEL) in log (mg/kg_bw/day) is provided in Tables 2a-2d. *Tetrahymena pyriformis* toxicity is employed as a toxic endpoint [29]. If the negative logarithm of the concentration required to inhibit 50% growth of *T. pyriformis* is greater than -0.5 log ug/L, then the compound is considered toxic [26]. Hence, all the tested oligosaccharides of different units were predicted to be toxic to *T. pyriformis.* Minnow toxicity signifies the lethal concentration values of a molecule that is required to cause the death of 50% of the Flathead Minnows. For a given compound, when the predicted log LC50 values are less than -0.3, the compound is observed to exhibit high acute toxicity [26]. This indicated that all the oligomeric molecules were non-toxic to minnows.

The bioactivity of carbohydrate-based molecules is promising to be used for various biomedical applications. These molecules also exhibit properties such as hydrophilicity and reduced toxicity, leading to enhanced bioavailability [30]. Ulvan, a polysaccharide obtained from Ulva sp., exhibits poor bioavailability, high molecular weight, and low solubility; it cannot be effectively utilized for various research purposes. But the oligosaccharides obtained from the degradation of ulvan showed enhanced bioavailability [31]. According to the literature, oligosaccharides from marine sources exhibit good bioavailability. Additionally, a redox-responsive delivery system based on colloidal mesoporous silica, along with an oligosaccharide of hyaluronic acid, utilizes disulfide bonds for targeted drug delivery against cancer cells [32]. Paclitaxel-loaded chitosan oligosaccharide-stabilized gold nanoparticles (PTX-COS AuNPs) were used for the targeted drug delivery to the cancer cells. These PTX-COS AuNPs showed pH-dependent drug release and strong anticancer activity against MDA-MB-231 cells [33]. Based on this delivery strategy, sulphated oligosaccharides can be encapsulated in nanomaterials for targeted drug delivery. Carbohydrate-based molecules such as lactulose have been used to treat chronic constipation [34], and heparin has been used clinically as an antithrombotic agent [35]. In recent decades, oligosaccharides have also been deliberated for their potential biological activities. Oligosaccharides such as fondaparinux (anticoagulant) and acarbose (α-glucosidase inhibitor for the treatment of diabetes) are currently used [36]. Oligosaccharides derived from seaweed have been approved for the treatment of Alzheimer's disease [37]. Heparin and related oligosaccharides were reported to exhibit anti-inflammatory and neuroprotective effects [38]. Non-Digestible Oligosaccharides were reported as therapeutic molecules against enterotoxin-producing bacteria and their toxins [39]. Oligosaccharides of HA were reported to be a potential anticancer drug [40]. Resveratrol

oligosaccharides are reported to exhibit anti- SARS-CoV-2 activity [41]. Oligosaccharides present in camel's milk have therapeutic potential to be used in the management of COVID-19 [42]. Sulphated polysaccharides such as heparin, heparin sulphate, other glycosaminoglycans (GAGs), and Fucoidan have better binding affinity with the SARS-CoV-2 spike protein, suggesting them to be used as an anti-viral agent [43]. Hence, these studies brighten the hope of endorsing carbohydrates, particularly oligosaccharides, in drug development and of directing efforts toward the development of carbohydrate-containing therapeutics in the near future.

Table 10. Toxicity analysis for oligosaccharides of 3 units.

S. no	Properties	Curdlan Sulfate	Curdlan	Fucoidan	Dextran sulfate	Lambda carrageenan	Kappa carrageenan	Dextran	Ulvan
1.	AMES toxicity (Yes/No)	No	No	No	No	No	No	No	No
2.	Max. tolerated dose (human) (log mg/kg/day)	0.438	0.185	0.224	0.445	-0.113	0.337	0.842	0.419
3.	hERG I inhibitor (Yes/No)	No	No	No	No	No	No	No	No
4.	hERG II inhibitor (Yes/No)	No	Yes	No	No	Yes	Yes	Yes	No
5.	Oral Rat Acute Toxicity (LD50) (mg/kg)	2482	2768	1571	1220	3004	2707	2614	2481
6.	Oral Rat Chronic Toxicity (LOAEL) (log mg/kg bw/day)	3774	3236	1650	2330	2876	4668	6641	6173
7.	Hepatotoxicity (Yes/No)	No	No	No	No	No	No	No	No
8.	Skin Sensitization (Yes/No)	No	No	No	No	No	No	No	No
9.	*T. pyriformis* toxicity (log ug/L)	0.285	0.285	0.393	0.285	0.285	0.285	0.285	0.285
10.	Minnow toxicity (log mM)	53.656	10.867	1.766	4.465	3.654	9.735	10.135	12.283

Table 11. Toxicity analysis for oligosaccharides of 4 units.

S. no	Properties	Curdlan Sulfate	Curdlan	Fucoidan	Dextran sulfate	Lambda carrageenan	Kappa carrageenan	Dextran	Ulvan
1.	AMES toxicity (Yes/No)	No	No	No	No	No	No	No	No
2.	Max. tolerated dose (human) (log mg/kg/day)	0.438	0.193	-0.589	0.438	-0.635	-0.494	0.43	0.435
3.	hERG I inhibitor (Yes/No)	No	No	No	No	No	No	No	No
4.	hERG II inhibitor (Yes/No)	No	Yes	No	No	Yes	Yes	Yes	No
5.	Oral Rat Acute Toxicity (LD50) (mg/kg)	2482	2727	4034	2482	3824	2815	2406	2482
6.	Oral Rat Chronic Toxicity (LOAEL) (log mg/kg_bw/day)	1099	3055	2279	6485	2144	4143	7452	5643
7.	Hepatotoxicity (Yes/No)	No	No	No	No	No	No	No	No
8.	Skin Sensitisation (Yes/No)	No	No	No	No	No	No	No	No
9.	*T. pyriformis* toxicity (log ug/L)	0.285	0.285	0.285	0.285	0.285	0.285	0.285	0.285
10.	Minnow toxicity (log mM)	21.49	14.678	5.137	84.431	4.206	11.135	15.872	13.658

Table 12. Toxicity analysis for oligosaccharides of 5 units.

S. no	Properties	Curdlan sulfate	Curdlan	Fucoidan	Dextran sulfate	Lambda carrageenan	Kappa carrageenan	Dextran	Ulvan
1.	AMES toxicity (Yes/No)	No	No	No	No	No	No	No	No
2.	Max. tolerated dose (human) (log mg/kg/day)	0.438	0.194	0.198	0.438	-0.436	-0.552	0.438	0.438
3.	hERG I inhibitor (Yes/No)	No	No	No	No	No	No	No	No
4.	hERG II inhibitor (Yes/No)	No	Yes	No	No	Yes	Yes	Yes	No
5.	Oral Rat Acute Toxicity (LD50) (mg/kg)	2482	2487	4361	2482	4258	2606	2459	2482
6.	Oral Rat Chronic Toxicity (LOAEL) (log mg/kg_bw/day)	1335	2971	2358	4283	2885	4789	8082	6322
7.	Hepatotoxicity (Yes/No)	No	No	No	No	No	No	No	No
8.	Skin Sensitisation (Yes/No)	No	No	No	No	No	No	No	No
9.	*T. pyriformis* toxicity (log ug/L)	0.285	0.285	0.285	0.285	0.285	0.285	0.285	0.285
10.	Minnow toxicity (log mM)	21.255	18.489	6.532	116.194	4.646	15.875	21.413	19.995

Table 13. Toxicity analysis for oligosaccharides of 10 units.

S. no	Properties	Curdlan sulfate	Curdlan	Fucoidan	Dextran Sulfate	Lambda carrageenan	Kappa carrageenan	Dextran	Ulvan
1.	AMES toxicity (Yes/No)	No	No	No	No	No	No	No	No
2.	Max. tolerated dose (human) (log mg/kg/day)	0.438	0.438	0.407	0.414	0.435	0.371	0.438	0.438
3.	hERG I inhibitor (Yes/No)	No	No	No	No	No	No	No	No
4.	hERG II inhibitor (Yes/No)	No	Yes	No	No	Yes	Yes	Yes	No
5.	Oral Rat Acute Toxicity (LD50) (mg/kg)	2482	2482	2814	2135	2486	2499	2482	2482
6.	Oral Rat Chronic Toxicity (LOAEL) (log mg/kg_bw/day)	1597	2554	0952	3125	3330	5772	1619	7653
7.	Hepatotoxicity (Yes/No)	No	No	Yes	No	No	No	No	No
8.	Skin Sensitisation (Yes/No)	No	No	No	No	No	No	No	No
9.	*T. pyriformis* toxicity (log ug/L)	0.285	0.285	0.285	0.285	0.285	0.285	0.285	0.285
10.	Minnow toxicity (log mM)	21.924	37.544	3.47	53.446	8.111	11.295	48.934	42.562

4. Conclusion

In this work, different oligosaccharides derived from bacterial and sulphated seaweed polysaccharides were assessed for their potential to inhibit SARS-CoV-2 proteins through in silico molecular docking analysis, and their toxicity was evaluated using the ADMET tool. From the docking studies, the 10 units of fucoidan oligomers showed higher binding scores with the nucleocapsid receptor-binding domains of COVID-19, followed by ulvan oligomers, compared to other sulphated oligosaccharides and the control drug. It was observed that the oligosaccharides have a higher binding affinity for the target COVID proteins than the control

drug. Further, the interacting amino acids differ across receptor-binding domains, and some residues are common across domains. Further, the toxicity properties of these oligosaccharides were assessed using various prediction parameters. The results indicate that the tested oligosaccharides possess favourable pharmacological properties, as inferred from in silico analysis. Therefore, these bioactive oligosaccharides can be exploited as an effective anti-viral therapeutic mediator for SARS-CoV-2, based on computational studies. Nevertheless, the efficacy must be supported by further in vitro and in vivo analyses.

Author Contributions

Conceptualization, A.R., G.P.S., and B.V.; methodology, A.R., G.P.S., and B.V.; software, A.R., G.P.S., and B.F.P.; validation, A.R., G.P.S., and B.F.P.; formal analysis, A.R., G.P.S., and B.V.; investigation, A.R., G.P.S., and B.V.; resources, B.V.; data curation, A.R. and B.V.; writing—original draft preparation, A.R. and G.P.S.; writing—review and editing, B.V.; visualization, A.R.; supervision, B.V.; project administration, B.V.; funding acquisition, B.V.; All authors have read and agreed to the published version of the manuscript.

Institutional Review Board Statement

Not applicable.

Informed Consent Statement

Not applicable.

Data Availability Statement

Data supporting the findings of this study are available upon reasonable request from the corresponding author.

Funding

This work was supported by the seed money grant from the management of Kalasalingam Academy of Research and Education (Grant number: KARE/VC/R&D/SMPG/2023-2024/01) to Vanavil Balakrishnan.

Acknowledgments

The University Research Fellowship provided by the management of Kalasalingam Academy of Research and Education to Aanandhalakshmi Raghuraman is gratefully acknowledged.

Conflicts of Interest

The authors declare that there is no conflict of interest.

References

1. Wang, J.; Zhang, Y.; Lu, Q.; Xing, D.; Zhang, R. Exploring Carbohydrates for Therapeutics: A Review on Future Directions. *Front. Pharmacol.* **2021**, *12*, 756724, https://doi.org/10.3389/fphar.2021.756724.
2. Michelle, K.; Lokesh, J. Carbohydrates in Therapeutics. *Cardiovasc. Hematol. Agents Med. Chem.* **2007**, *5*, 186-197, https://doi.org/10.2174/187152507781058663.

3. Hosen, M.A.; El Bakri, Y.; Rehman, H.M.; Hashem, H.E.; Saki, M.; Kawsar, S.M.A. A computational investigation of galactopyranoside esters as antimicrobial agents through antiviral, molecular docking, molecular dynamics, pharmacokinetics, and bioactivity prediction. *J. Biomol. Struct. Dyn.* **2024**, *42*, 1015-1030, https://doi.org/10.1080/07391102.2023.2198606.
4. Lam, K.-L.; Cheung, P.C.-K. Carbohydrate-Based Prebiotics in Targeted Modulation of Gut Microbiome. *J. Agric. Food Chem.* **2019**, *67*, 12335-12340, https://doi.org/10.1021/acs.jafc.9b04811.
5. Okechukwu, Q.N.; Adepoju, F.O.; Kanwugu, O.N.; Adadi, P.; Serrano-Aroca, Á.; Uversky, V.N.; Okpala, C.O.R. Marine-Derived Bioactive Metabolites as a Potential Therapeutic Intervention in Managing Viral Diseases: Insights from the SARS-CoV-2 In Silico and Pre-Clinical Studies. *Pharmaceuticals* **2024**, *17*, 328, https://doi.org/10.3390/ph17030328.
6. Hans, N.; Gupta, S.; Patel, A.K.; Naik, S.; Malik, A. Deciphering the role of fucoidan from brown macroalgae in inhibiting SARS-CoV-2 by targeting its main protease and receptor binding domain: *Invitro* and *insilico* approach. *Int. J. Biol. Macromol.* **2023**, *248*, 125950, https://doi.org/10.1016/j.ijbiomac.2023.125950.
7. Lai, S.; Yang, C.; Liu, S.; Yuan, S.; Liu, Y.; Yan, X.; Zhao, C. Biological activities and potential therapeutic applications of functional oligosaccharides. *MOJ Food Process. Technol.* **2017**, *5*, 245-248, https://doi.org/10.15406/mojfpt.2017.05.00119.
8. Yu, M.; Zhang, T.; Zhang, W.; Sun, Q.; Li, H.; Li, J.-p. Elucidating the Interactions Between Heparin/Heparan Sulfate and SARS-CoV-2-Related Proteins—An Important Strategy for Developing Novel Therapeutics for the COVID-19 Pandemic. *Front. Mol. Biosci.* **2021**, *7*, 628551, https://doi.org/10.3389/fmolb.2020.628551.
9. Cao, X.; Du, X.; Jiao, H.; An, Q.; Chen, R.; Fang, P.; Wang, J.; Yu, B. Carbohydrate-based drugs launched during 2000−2021. *Acta Pharm. Sin. B* **2022**, *12*, 3783-3821, https://doi.org/10.1016/j.apsb.2022.05.020.
10. Tate, P.M.; Mastrodomenico, V.; Cunha, C.; McClure, J.; Barron, A.E.; Diamond, G.; Mounce, B.C.; Kirshenbaum, K. Peptidomimetic Oligomers Targeting Membrane Phosphatidylserine Exhibit Broad Antiviral Activity. *ACS Infect. Dis.* **2023**, *9*, 1508-1522, https://doi.org/10.1021/acsinfecdis.3c00063.
11. Min, Y.-Q.; Duan, X.-C.; Zhou, Y.-D.; Kulinich, A.; Meng, W.; Cai, Z.-P.; Ma, H.-Y.; Liu, L.; Zhang, X.-L.; Voglmeir, J. Effects of microvirin monomers and oligomers on hepatitis C virus. *Biosci. Rep.* **2017**, *37*, BSR20170015, https://doi.org/10.1042/BSR20170015.
12. Cheong, K.-L.; Chen, S.; Teng, B.; Veeraperumal, S.; Zhong, S.; Tan, K. Oligosaccharides as Potential Regulators of Gut Microbiota and Intestinal Health in Post-COVID-19 Management. *Pharmaceuticals* **2023**, *16*, 860, https://doi.org/10.3390/ph16060860.
13. Mahaboob Ali, A.A.; Vishal, A.; Nelson, E.J.R. Targeting host-virus interactions: in silico analysis of the binding of human milk oligosaccharides to viral proteins involved in respiratory infections. *Sci. Rep.* **2024**, *14*, 4111, https://doi.org/10.5281/zenodo.10440575.
14. Rohilla, D.; Srivastava, A.K.; Singh, R.P.; Yadav, P.; Singh, S.K.; Kumar, D.; Bhardwaj, N.; Kesawat, M.S.; Pandey, K.D.; Kumar, A. Algae Polysaccharides (Carrageenan and Alginate)—A Treasure-Trove of Antiviral Compounds: An In Silico Approach to Identify Potential Candidates for Inhibition of S1-RBD Spike Protein of SARS-CoV2. *Stresses* **2023**, *3*, 555-569, https://doi.org/10.3390/stresses3030039.
15. Senan, A.M.; Muhammed, M.T.; Akkoc, S.; Alhag, S.K.; Al-Shahari, E.A.; Al-Shuraym, L.A. Modification of ionic liquid and lactoferrin-based small molecules as potential therapeutics against SARS-CoV-2: Molecular docking disclosed the predictable results. *J. Mol. Struct.* **2025**, *1319*, 139353, https://doi.org/10.1016/j.molstruc.2024.139353.
16. Almeida, B.; Domingues, C.; Mascarenhas-Melo, F.; Silva, I.; Jarak, I.; Veiga, F.; Figueiras, A. The Role of Cyclodextrins in COVID-19 Therapy—A Literature Review. *Int. J. Mol. Sci.* **2023**, *24*, 2974, https://doi.org/10.3390/ijms24032974.
17. Verma, A.; Adhikary, A.; Woloschak, G.; Dwarakanath, B.S.; Papineni, R.V.L. A combinatorial approach of a polypharmacological adjuvant 2-deoxy-D-glucose with low dose radiation therapy to quell the cytokine storm in COVID-19 management. *Int. J. Radiat. Biol.* **2020**, *96*, 1323-1328, https://doi.org/10.1080/09553002.2020.1818865.
18. Pereira, L.; Critchley, A.T. The COVID 19 novel coronavirus pandemic 2020: seaweeds to the rescue? Why does substantial, supporting research about the antiviral properties of seaweed polysaccharides seem to go unrecognized by the pharmaceutical community in these desperate times?. *J. Appl. Phycol.* **2020**, *32*, 1875-1877, https://doi.org/10.1007/s10811-020-02143-y.

19. Pashameah, R.A.; Soltane, R.; Sayed, A.M. A novel inhibitor of SARS-CoV infection: Lactulose octasulfate interferes with ACE2-Spike protein binding. *Heliyon* **2024**, *10*, e23222, https://doi.org/10.1016/j.heliyon.2023.e23222.
20. Geng, L.; Zhang, Q.; Suo, Q.; Wang, J.; Wang, Y.; Wang, C.; Wu, N. Inhibitory activity of a sulfated oligo-porphyran from *Pyropia yezoensis* against SARS-CoV-2. *Carbohydr. Polym.* **2023**, *299*, 120173, https://doi.org/10.1016/j.carbpol.2022.120173.
21. Pham, H.T.N.; Phung, H.T.T. Comparing the performance of molecular docking tools for HIV-1 protease inhibitors. *J. Adv. Eng. Comput.* **2023**, *7*, 95-104, https://doi.org/10.55579/jaec.202372.400.
22. Pokharkar, O.; Anumolu, H.; Zyryanov, G.V.; Tsurkan, M.V. Natural Products from Red Algal Genus *Laurencia* as Potential Inhibitors of RdRp and nsp15 Enzymes of SARS-CoV-2: An In Silico Perspective. *Microbiol. Res.* **2023**, *14*, 1020-1048, https://doi.org/10.3390/microbiolres14030069.
23. Choudhary, S.; Malik, Y.S.; Tomar, S. Identification of SARS-CoV-2 Cell Entry Inhibitors by Drug Repurposing Using in silico Structure-Based Virtual Screening Approach. *Front. Immunol.* **2020**, *11*, 1664, https://doi.org/10.3389/fimmu.2020.01664.
24. Lagorce, D.; Douguet, D.; Miteva, M.A.; Villoutreix, B.O. Computational analysis of calculated physicochemical and ADMET properties of protein-protein interaction inhibitors. *Sci. Rep.* **2017**, *7*, 46277, https://doi.org/10.1038/srep46277.
25. Pham-Khanh, N.-H.; Ha, T.-K.-Q.; Duong, K.-V. Bifunctional neuraminidase inhibitory and simultaneously anti-*Mycoplasma pneumoniae* of flavan-3-ols and flavanones: Combined molecular docking, virtual screening, ADMET, and synthesis prediction. *J. King Saud Univ. Sci.* **2024**, *36*, 103242, https://doi.org/10.1016/j.jksus.2024.103242.
26. Li, B.; Zhang, T.; Cao, H.; Ferro, V.; Li, J.; Yu, M. Identification of a Pentasaccharide Lead Compound with High Affinity to the SARS-CoV-2 Spike Protein via In Silico Screening. *Int. J. Mol. Sci.* **2023**, *24*, 16115, https://doi.org/10.3390/ijms242216115.
27. Pires, D.E.V.; Blundell, T.L.; Ascher, D.B. pkCSM: Predicting Small-Molecule Pharmacokinetic and Toxicity Properties Using Graph-Based Signatures. *J. Med. Chem.* **2015**, *58*, 4066-4072, https://doi.org/10.1021/acs.jmedchem.5b00104.
28. Bhat, V.; Chatterjee, J. The Use of *In Silico* Tools for the Toxicity Prediction of Potential Inhibitors of SARS-CoV-2. *ATLA - Altern. Lab. Anim.* **2021**, *49*, 22-32, https://doi.org/10.1177/02611929211008196.
29. Cheng, F.; Shen, J.; Yu, Y.; Li, W.; Liu, G.; Lee, P.W.; Tang, Y. *In silico* prediction of *Tetrahymena pyriformis* toxicity for diverse industrial chemicals with substructure pattern recognition and machine learning methods. *Chemosphere* **2011**, *82*, 1636-1643, https://doi.org/10.1016/j.chemosphere.2010.11.043.
30. Mishra, S.; Upadhaya, K.; Mishra, K.B.; Shukla, A.K.; Tripathi, R.P.; Tiwari, V.K. Chapter 10 - Carbohydrate-Based Therapeutics: A Frontier in Drug Discovery and Development. In Studies in Natural Products Chemistry, Atta ur, R., Ed.; Elsevier: **2016**; Volume 49, pp. 307-361, https://doi.org/10.1016/B978-0-444-63601-0.00010-7.
31. Li, C.; Tang, T.; Du, Y.; Jiang, L.; Yao, Z.; Ning, L.; Zhu, B. Ulvan and *Ulva* oligosaccharides: a systematic review of structure, preparation, biological activities and applications. *Bioresour. Bioprocess.* **2023**, *10*, 66, https://doi.org/10.1186/s40643-023-00690-z.
32. Zhao, Q.; Geng, H.; Wang, Y.; Gao, Y.; Huang, J.; Wang, Y.; Zhang, J.; Wang, S. Hyaluronic Acid Oligosaccharide Modified Redox-Responsive Mesoporous Silica Nanoparticles for Targeted Drug Delivery. *ACS Appl. Mater. Interfaces* **2014**, *6*, 20290-20299, https://doi.org/10.1021/am505824d.
33. Manivasagan, P.; Bharathiraja, S.; Bui, N.Q.; Lim, I.G.; Oh, J. Paclitaxel-loaded chitosan oligosaccharide-stabilized gold nanoparticles as novel agents for drug delivery and photoacoustic imaging of cancer cells. *Int. J. Pharm.* **2016**, *511*, 367-379, https://doi.org/10.1016/j.ijpharm.2016.07.025.
34. Liu, L.W.C. Chronic Constipation: Current Treatment Options. *Can. J. Gastroenterol. Hepatol.* **2011**, *25*, 360463, https://doi.org/10.1155/2011/360463.
35. Blann, A.D.; Landray, M.J.; Lip, G.Y.H. An overview of antithrombotic therapy. *BMJ* **2002**, *325*, 762, https://doi.org/10.1136/bmj.325.7367.762.
36. Ernst, B.; Magnani, J.L. From carbohydrate leads to glycomimetic drugs. *Nat. Rev. Drug Discov.* **2009**, *8*, 661-677, https://doi.org/10.1038/nrd2852.
37. Wang, X.; Sun, G.; Feng, T.; Zhang, J.; Huang, X.; Wang, T.; Xie, Z.; Chu, X.; Yang, J.; Wang, H.; Chang, S.; Gong, Y.; Ruan, L.; Zhang, G.; Yan, S.; Lian, W.; Du, C.; Yang, D.; Zhang, Q.; Lin, F.; Liu, J.; Zhang, H.; Ge, C.; Xiao, S.; Ding, J.; Geng, M. Sodium oligomannate therapeutically remodels gut microbiota and

suppresses gut bacterial amino acids-shaped neuroinflammation to inhibit Alzheimer's disease progression. *Cell Res.* **2019**, *29*, 787-803, https://doi.org/10.1038/s41422-019-0216-x.
38. Qing, M.; Umberto, C.; Israel, H.; Walter, P.J.; Robert, J.L.; Jeanine, M.W.; Jawed, F.; John, M.L. Heparin Oligosaccharides as Potential Therapeutic Agents in Senile Dementia. *Curr. Pharm. Des.* **2007**, *13*, 1607-1616, https://doi.org/10.2174/138161207780765918.
39. Asadpoor, M.; Ithakisiou, G.-N.; Henricks, P.A.J.; Pieters, R.; Folkerts, G.; Braber, S. Non-Digestible Oligosaccharides and Short Chain Fatty Acids as Therapeutic Targets against Enterotoxin-Producing Bacteria and Their Toxins. *Toxins* **2021**, *13*, 175, https://doi.org/10.3390/toxins13030175.
40. Bryan, P.T.; Shibnath, G.; Suniti, M. Hyaluronan Oligosaccharides as a Potential Anticancer Therapeutic. *Curr. Pharm. Biotechnol.* **2008**, *9*, 249-252, https://doi.org/10.2174/138920108785161569.
41. Hamada, H.; Hamada, H.; Shimoda, K.; Kuboki, A.; Iwaki, T.; Kiriake, Y.; Ishihara, K. Resveratrol Oligosaccharides (Gluco-Oligosaccharides) Effectively Inhibit SARS-CoV-2 Infection: Glycoside (Polysaccharide) Approach for Treatment of COVID-19. *Nat. Prod. Commun.* **2021**, *16*, 1934578X211012903, https://doi.org/10.1177/1934578X211012903.
42. Mourad, E. Milk Oligosaccharides and Lectins as Candidates for Clinical Trials against Covid-19. *Curr. Nutr. Food Sci.* **2021**, *17*, 246-248, https://doi.org/10.2174/1573401316999200819125355.
43. Kwon, P.S.; Oh, H.; Kwon, S.-J.; Jin, W.; Zhang, F.; Fraser, K.; Hong, J.J.; Linhardt, R.J.; Dordick, J.S. Sulfated polysaccharides effectively inhibit SARS-CoV-2 in vitro. *Cell Discov.* **2020**, *6*, 50, https://doi.org/10.1038/s41421-020-00192-8.

Publisher's Note & Disclaimer